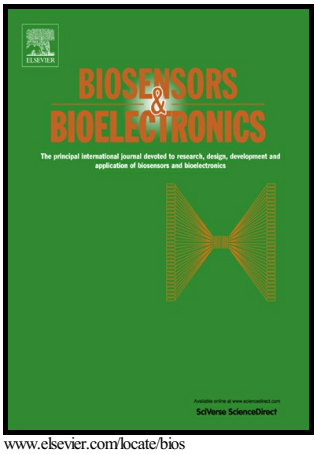

www.elsevier.com/locate/bios

Ultrasensitive Electrochemiluminescence Biosensor for Detection of Laminin Based on DNA Dendrimer-Carried Luminophore and DNA Nanomachine-Mediated Target Recycling Amplification

Li Li, Changchun Niu, Tian Li, Yafang Wan, Ying Zhou, Haijun Wang, Ruo Yuan, Pu Liao

PII: S0956-5663(17)30668-1
DOI: https://doi.org/10.1016/j.bios.2017.10.009
Reference: BIOS10034

To appear in: *Biosensors and Bioelectronic*

Received date: 20 July 2017
Revised date: 24 September 2017
Accepted date: 2 October 2017

Cite this article as: Li Li, Changchun Niu, Tian Li, Yafang Wan, Ying Zhou, Haijun Wang, Ruo Yuan and Pu Liao, Ultrasensitive Electrochemiluminescence Biosensor for Detection of Laminin Based on DNA Dendrimer-Carried Luminophore and DNA Nanomachine-Mediated Target Recycling Amplification, *Biosensors and Bioelectronic,* https://doi.org/10.1016/j.bios.2017.10.009

Ultrasensitive Electrochemiluminescence Biosensor for Detection of Laminin Based on DNA Dendrimer-Carried Luminophore and DNA Nanomachine-Mediated Target Recycling Amplification

Li Li[a,1], Changchun Niu[a,1], Tian Li[a], Yafang Wan[a], Ying Zhou[b], Haijun Wang[b], Ruo Yuan[b], Pu Liao[a,*]

[a]*Department of Laboratory Medicine, Chongqing General Hospital, Chongqing 400014, China*

[b]*Key Laboratory of Luminescent and Real-Time Analytical Chemistry (Southwest University), Ministry of Education, College of Chemistry and Chemical Engineering, Southwest University, Chongqing 400715, China*

Abstract

Herein, a novel electrochemiluminescence (ECL) biosensor was proposed for ultrasensitive detection of laminin (LN), in which DNA dendrimer (D) as a promising nanocarrier for luminophore and DNA nanomachine as tactic for target recycling. The DNA dendrimer was synthesized by hybridization between sense and its antisense Y-shaped DNAs which were formed via reaction between single-stranded DNA (ssDNA) with a thiol group at the 5'-end and a synthesized trimeric cross-linker of tris(2-maleimidoethyl)amine. This dendrimer provided abundant double-stranded DNA (dsDNA) to achieve high loading efficiency for ECL luminophore. Simultaneously, N-(aminobutyl)-N-(ethylisoluminol) (ABEI) was conjugated with

doxorubicin (Dox, a intercalator of dsDNA) to form the ECL indicator (Dox-ABEI) which could effectively intercalate DNA dendrimer to form the ECL probe (D-Dox-ABEI). Subsequently, a DNA nanomachine activated by target protein was involved to obtain numerous output ssDNA (S2) which was amplified by exonuclease III-assisted recycle and immobilized on ssDNA (S1)-modified sensing electrode surface via complementation. Thereby, abundant D-Dox-ABEI probes were captured by S2 to construct the biosensor for target protein detection. The proposed ECL biosensor realized the ultrasensitive detection of LN with a linear range from 0.1 pg/mL to 100 ng/mL and a low detection limit of 0.0661 pg/mL. Impressively, the application of this ECL biosensor would provide the great potential for analysis of other proteins, revealing a new avenue for early diagnosis and the prognosis evaluation of various diseases.

Keywords: DNA dendrimer; DNA nanomachine; Electrochemiluminescence biosensor; Laminin

* Corresponding author. Tel: +86-23-63516362; Fax: +86-23-63516241.

E-mail address: liaopu2015@163.com

[1] These authors contributed equally to this work.

1. Introduction

Immobilization strategies of luminophores have attracted explosive interest in electrochemiluminescence (ECL) systems because they could enhance the luminous efficiency significantly by shortening electron-transfer path (Jiang et al., 2015; Li et

al., 2015; Zhang et al., 2015; Zhang et al., 2016). However, in most conventional immobilization methods, metal nanoparticles as carriers exhibited the inherent toxicity, which limited their applications in bioassays (Jiang et al., 2016; Liu et al., 2016; Wang et al., 2015). Currently, the self-assembled DNA nanostructures with different shapes have been one of the most promising research areas because of their low toxicity and excellent biocompatibility (Bi et al., 2015; Sadowski et al., 2014; Zhou et al., 2012; Mohammed and Schulman., 2013; Xie et al., 2016; Endo et al., 2010). Tan's group reported the self-assembly of multifunctional DNA nanoflowers for selective cancer cell recognition, bioimaging, and targeted anticancer drug delivery (Zhu et al., 2013). A DNA dendrimer scaffold was constructed by Meng and coworkers, which was used as an efficient nanocarrier to deliver functional nucleic acids and in situ monitor biological molecules in living cells (Meng et al., 2014). The large specific surface area, good stability, high branch and excellent monodispersity, made DNA dendrimers more advantageous than other nanocarriers, which have been widely applied in much biomedical analysis (Liu et al., 2015; Zhao et al., 2015; Zhang et al., 2015; Zhu et al., 2013). Recently, we used tetrahedron DNA dendrimers and biotin labeled DNA dendrimer as nanocarriers to provide sufficient intercalated sites for ECL luminophores, resulting in ultrasensitive detection of biological active substances (Xie et al., 2016; Wang et al., 2016). Despite the immobilization of luminophores has been improved, these DNA dendrimers were still confronted with some limitations of complicated operation, variety DNA strands and insufficient specific surface area. In this perspective, seeking a high-efficient DNA dendrimer

with simple preparation process to load luminophores for significantly promoting luminescence remains a realistic challenge in ECL biosensor construction. Recently, dendrimer-like polymeric DNAs was prepared for analysis of telomere DNA by El-Mahdy and coworkers (El-Mahdy et al., 2014), which could be acted as a particularly promising nanocarrier for binding of the luminophores because of its simple preparation process, sufficient hydrogen bonds and high specific surface.

The detection of proteins plays the key roles in early clinical diagnosis and disease prevention. Xing's group reported the detection of protein by aptamer-based ECL method (Zhou et al., 2014; Zhu et al., 2012; Zhu et al., 2010). Recently, various DNA nanomachines have been constructed based on the exquisite specificity, predictability and diversity of DNA hybridization (Wang et al., 2015; Zhou et al., 2012; Xu et al., 2015; Lund et al., 2010; Zhang et al., 2014). Significantly, these DNA nanomachines have aroused widespread attention due to easy operation, isothermal reaction, good reversible, high sensitivity, repeatable mechanical motion and three-dimensional DNA tracks (Li et al., 2016; Xu et al., 2015; Liber et al., 2015; Muscat et al., 2012; Jiang et al., 2017). In recent years, DNA nanomachines have been widely used with signal amplification strategies for detection of various targets (Liu et al., 2015; Wang et al., 2013; Zong et al., 2015; Yang et al., 2016; Zhang et al., 2015). Li's group reported an enzyme-powered DNA nanomachine based on a DNA-functionalized gold nanoparticle, which moves a DNA walker along a three-dimensional DNA track and executes the task of releasing payloads (Yang et al., 2016). Zhang and coworkers introduced binding-induced DNA nanomachines that

were specifically activated by streptavidin, platelet-derived growth factor, and the smallpox gene (Zhang et al., 2015). Inspired by the above application of the nanomachines, a promising immunoreaction-induced DNA nanomachine was constructed to achieve ultrasensitive detection of target proteins, in which the input target protein could be converted to unique output ssDNA and this process could be amplified by enzyme-assisted target recycling.

A proposed ECL biosensor based on a DNA dendrimer-carried luminescent system and DNA nanomachine-mediated target recycling amplification was fabricated for ultrasensitive detection of laminin (LN), one of the main glycoproteins of the basement membrane, and exerted many important functions in a series of such biological phenomena as adhesion, migration, cellular differentiation and growth (Kleinman et al., 1985; Valkonen et al., 1993), which was an efficient and widely used biomarker of liver fibrosis (Li et al., 2012; El-Mezayen et al., 2015; Rodin et al., 2010). Herein, a DNA dendrimer (D) with sufficient intercalated sites was prepared by hybridization between Y-shaped ssDNA (Y1) and its antisense Y-shaped cDNA (Y2). N-(aminobutyl)-N-(ethylisoluminol) (ABEI) as a derivative of luminol, was conjugated with doxorubicin (Dox), an intercalator of double stranded DNA, to form the ECL indicator (Dox-ABEI), which was non-covalently intercalated in DNA dendrimer, forming the ECL probe (D-Dox-ABEI) with improved luminous efficiency. Subsequently, hundreds of DNA3 and tens of DNA1 were immobilized on surface of gold nanoparticle (AuNP), and then capture antibody (Ab1) was conjugated on the free end of DNA1 by amide linkage. The short sequence S2 (complementary strand of

DNA3), Ab2-modified DNA2 (DNA2-Ab2) and exonuclease III (Exo III) were added in above solution to prepare the DNA nanomachine for improving the sensitivity of detection. As exhibited in Scheme 1, the bare glassy carbon electrode (GCE) was deposited with L-cysteine (L-Cys) and gold chloride tetrahydrate ($HAuCl_4 \cdot 4H_2O$) successively to obtain GCE/L-Cys/AuNPs platform, which could further enhance the luminous efficiency of ABEI and immobilize more thiol modified capture probe (S1) via Au-S covalent bond. In the presence of target LN, sandwich immunoreaction would activate DNA nanomachine to displace S2 from S2/DNA3 duplex with formation of DNA2/DNA3. To enhance the conversion ratio, Exo III was used to digest the 3′ recessed DNA3 strand in the DNA2/DNA3 duplex with release of DNA2, which could initiate another reaction cycle again to displace more S2. Therefore, a target protein molecule of LN input could induce more than one S2 output as bridge to connect modified electrode and ECL probe for enhancing the detection sensitivity significantly. In this work, a DNA dendrimer was prepared as a powerful carrier for luminophores because of its simple preparation steps, large specific surface, as well as numerous hydrogen bonding sites. Meanwhile, the target LN circularly activated the DNA nanomachine, which realized circle amplification and ultrasensitive detection of target protein. The successful establishment of the ECL biosensor offered an efficient strategy for the ultrasensitive detection of LN without any expensive setup and tedious processes, which could be readily expanded for the detection of various kinds of biomarker proteins, revealing a new avenue for early disease diagnosis with higher efficiency.

Scheme 1.

2. Experiment Section

2.1. Materials and reagents

Tris (2-maleimidoethyl) amine (TMEA) was obtained from Tianjin Heowns Biochem LLC (Tianjin, China). Doxorubicin hydrochloride (Dox), N-(4-aminobutyl)-N-(ethylisoluminol) (ABEI), gold chloride tetrahydrate ($HAuCl_4 \cdot 4H_2O$) and hexanethiol (HT) were purchased from Sigma-Aldrich Co. (St Louis, MO, USA). Dithiothreitol (DTT), L-Cysteine (L-Cys), N-(3-(dimethylamino)propyl)-N-ethylcarbodiimide hydrochloride (EDC), N-hydroxy succinimide (NHS) and glutaraldehyde (GA) were obtained from Shanghai Medpep Co. Ltd. (Shanghai, China). Sodium hydroxide (NaOH), H_2O_2 (30%) and other reagents were supplied by Chemical Reagent Co. (Chongqing, China).

All the synthetic DNA sequences employed in this work (displayed in Table S1) were purchased from Shanghai Sangon Biological Engineering Technology & Services Co., Ltd. (Shanghai, China). Exonuclease III (Exo III) was obtained from New England Biolabs Ltd. (Beijing, China). Human Laminin (LN) and mucin 1 (MUC 1) ELISA Kits were purchased from Shanghai HuaYi Bio-technology Co. Ltd (Shanghai, China). Carcinoembryonic antigen (CEA) and α-1-fetoprotein (AFP) ELISA Kits were obtained from Biocell Co. (Zhengzhou, China). The human serum samples used in this work were provided by Chongqing General Hospital (Chongqing, China). The buffers employed in the research were showing as follows: 1× Tris-EDTA buffer (TE, containing 10 mM Tris-HCl, 1 mM ethylenediaminetetraacetic acid

(EDTA), pH 8.0) was used to dissolve the oligonucleotides; DNA hybridization buffer (HB, containing 10 mM Tris-HCl, 1 mM EDTA, and 1 M NaCl, pH 7.0) was used as binding solution for DNA hybridization; pH 7.0); Tris (hydroxymethyl) aminomethane-hydrochloride (Tris-HCl, 20 mM, containing 140 mM NaCl, 5 mM KCl, 1 mM $CaCl_2$, and 1 mM $MgCl_2$, pH 7.4) was employed as the binding buffer; phosphated buffered solution (PBS, 0.1 M, containing 10 mM KCl and 2 mM $MgCl_2$, pH 8.0 and pH 8.5) was employed as the working buffer solution (all PBS were air-saturated unless otherwise specified). All solutions were stored in the refrigerator (4 °C). Ultrapure water (specific resistance of 18.2 MΩ cm) was used throughout this experiment. All chemicals were of analytical grade and used as received without further purification.

2.2. Apparatus

Cyclic voltammetric (CV), electrochemical impedance spectroscopy (EIS), and electrochemical deposition were carried out with a CHI 660E electrochemistry workstation (Shanghai Chenhua Instrument, Shanghai, China). The ECL emissions were monitored with a MPI-A ECL analyzer (Xi'an Remax Electronic Science & Technology Co. Ltd, Xi'an, China), which used a conventional three-electrode system (modified glassy carbon electrode (GCE Φ = 4 mm) as the working electrode, platinum wire as the counter electrode, and Ag/AgCl (sat. KCl) as the reference electrode). The polyacrylamide gel electrophoresis (PAGE) was stained with a fluorescent dye, SYBR-Gold. Each band intensity was calculated by a densitometry using Image J software (Bio-Rad, Hercules, CA). For characterization, scanning

electron microscopy (SEM, Hitachi, Japan) and atomic force microscopy (AFM, Bruker Co., USA) were used. The UV-vis absorption spectra were obtained with a UV-2450 spectrophotometer (Shimadzu, Tokyo, Japan).

2.3. Preparation of the DNA dendrimer

The DNA dendrimer (D) was prepared via self-assembly of two complete complementary sequences modified by TMEA (a trimeric cross-linker) according to the reference (El-Mahdy et al., 2014) with slight modification shown in Fig. S1. First, the thiol-blocked sense or antisense DNA (DNA or cDNA) at 5'-end was incubated with DTT (50 mM) in PBS (100 μL, pH 8.5) at room temperature for 1 h to produce free thiol group, and then reacted with TMEA at a molar concentration ratio of 3:1 in Tris-HCl to form Y-shaped single-stranded DNA (Y1 or its antisense Y2) with a final concentration of 4 μM respectively. After overnight incubation at room temperature, the residual TMEA was eliminated by the NAP-10 column. Then, equal amounts of Y1 and Y2 were incubated in Tris-HCl at 37 °C for 1 h to produce the carrier of DNA dendrimer via self-assembly.

2.4. Preparation of the D-Dox-ABEI complex

The manufacturing process of D-Dox-ABEI complex was shown in Scheme 1A. Firstly, the Dox-ABEI complex prepared according to a previous report (Xie et al., 2016) with some modification (shown in Fig. S3). Secondly, 1 mL of the Dox-ABEI complex was added into the above DNA dendrimer solution (2 μM, 0.5 mL) and stored for 4 h at room temperature for noncovalently attach to dsDNA adequately

through intercalation. Ultimately, the above mixture was transferred into a dialysis tube and dialyzed for 1 day to remove uncombined Dox-ABEI complex with mild shaking to obtain D-Dox-ABEI complex.

2.5. Fabrication of an immunoreaction-induced DNA nanomachine for LN assay

The fabrication of an immunoreaction-induced DNA nanomachine for LN assay was showed in Scheme 1B. Firstly, the AuNPs (with an average diameter of 16 ± 5 nm) were prepared by citrate reduction of $HAuCl_4{\cdot}4H_2O$ according to the classic procedure with certain modifications and the morphologies were shown in Fig. S4A. Secondly, thiol-modified single-stranded DNA1 (2 μM) and DNA3 (20 μM) which served as the scaffold and separator for the protein conversion were reacted with AuNPs (1% w/w) in 100 μL of Tris-HCl buffer for 16 h at room temperature, and the supernatant was removed by centrifugation. Then the centrifugal product was dispersed in 100 μL of Tris-HCl buffer, followed by adding EDC (20 mM) and NHS (5 mM) to activate the carboxyl group of DNA1, and HT (1 mM) to block nonspecific binding sites. Subsequently, Ab1 (50 μL, 4 μM) and S2 (50 μL, 4 μM, hybridized to DNA3 with formation of S2/DNA3 duplex) were added and incubated for 12 h, thus, the DNA1-Ab1 and S2/DNA3 duplex could be formed on the surface of AuNPs. The unreacted S2 and Ab1 were removed by centrifugation. Then DNA2-Ab2 (20 μL, shown in Fig. S5), Exo III (300 U/mL) and LN solution (40 μL) with various concentrations were added into the complex and reacted at 37 °C for 2 h.

The operation mechanism of DNA nanomachine was illustrated in Fig. S2. In the absence of target LN, the displacement of S2 by DNA2 is minimal. However, when

LN existed, the sandwich immunoreaction would activate DNA nanomachine which brought DNA2 into close proximity to the S2/DNA3 duplex and then accelerated the strand-displacement reaction between DNA2 and S2 with formation of DNA2/DNA3 and release of S2. Finally, the solution containing various concentrations of S2 could be collected after centrifugation and used for triggering D-Dox-ABEI complex assembly on the surface of electrode by the complementary base pairing.

2.6. Construction of the ECL biosensor

The construction of the ECL biosensor for LN detection was presented in Scheme 1C. First of all, the GCE (Φ = 4 mm) was rinsed and sonicated with ethanol and ultrapure water respectively, then polished with 0.3 and 0.05 μm Al_2O_3 slurry orderly. Subsequently, the polished GCE was immersed in 2 mL of solution containing L-Cys (0.02 M) and HCl (0.1 M) with cyclic voltammetry deposition under the potential from -0.5 to 1.0 V for 15 cycles to obtain a porous L-Cys film modified electrode (GCE/L-Cys). Next, the GCE/L-Cys was immersed into $HAuCl_4{\cdot}4H_2O$ (1%) solution, and then electrodeposited at -0.2 V for 30 s to obtain an AuNPs layer on the surface of L-Cys to form the GCE/L-Cys/AuNPs (Fig. S4B). Next, single-stranded S1 (1.0 μM) was incubated on the surface of GCE/L-Cys/AuNPs via Au-S bond at 4 °C overnight. After rinsing, HT (1 mM) was cast onto the GCE/L-Cys/AuNPs/S1 for 30 min at room temperature for blocking the nonspecific recognition sites. After rinsing, different concentrations of S2 (10 μL) produced by DNA nanomachine were placed onto the GCE/L-Cys/AuNPs/S1/HT for 2 h at room temperature. After that, the prepared D-Dox-ABEI complex was captured

through the specific base pairing with the S2/S1 for 4 h at room temperature. Ultimately, the prepared biosensor was used for ECL detection and stored in 4 °C when not in use.

2.7. ECL detection procedure

After the modified electrode (GCE/L-Cys/AuNPs/S1/HT/S2) was incubated with D-Dox-ABEI complex for 4 h at room temperature, it was rinsed thoroughly by ultrapure water to remove the redundant D-Dox-ABEI complex. The obtained biosensor was detected in the buffer of 2 mL PBS (0.1 M, pH 8.0) containing H_2O_2 (2 mM) at room temperature to investigate the ECL response. The ECL intensity was gained by a MPI-A ECL analyzer with working potential from 0 V to 0.6 V (vs. Ag/AgCl) at a scan rate of 0.1 V/s, and the voltage of the photomultiplier tube (PMT) at 800 V.

3. Results and discussion

3.1. Characterization of DNA dendrimer

The DNA, cDNA, Y1, Y2 and D were analyzed using 20% PAGE shown in Fig. 1A, the single-stranded DNA (lane 1) and its antisense cDNA (lane 3) with the lowest molecular weight ran fastest on the gel, which reacted with TMEA to form the sense Y-shaped single-stranded DNA (Y1, lane 2) and its antisense Y-shaped single-stranded cDNA (Y2, lane 4) in the shape of trimeric, dimeric and monomeric DNAs on the gel. Then these Y-shaped DNAs could hybridize with each other to produce the three-dimensional meshy DNA dendrimers (D) with the largest molecular weight ran slowest on the gel (lane 5). Moreover, AFM (Fig. 1B) and SEM (Fig. 1C) were further

employed to observe the size and morphology of the assembled DNA dendrimer, which showed nearly spherical morphology with an average diameter of 300 ± 50 nm. These results suggested the successful formation of the DNA dendrimer.

Fig. 1.

3.2. Stepwise characterization of the proposed ECL biosensor

CV and EIS were employed to confirm the process of the biosensor fabrication in $[Fe(CN)_6]^{3-/4-}$ (5.0 mM) containing KCl (0.1 M). As displayed in Fig. 2A, an initial CV peak was acquired on the pretreated bare GCE (curve a). After L-Cys was deposited onto electrode, the peak current decreased owing to the suppression of L-Cys for electron transmission (curve b). After AuNPs were electrodeposited onto the electrode surface, the peak current increased because of the excellent conductivity of AuNPs (curve c). After the S1 was immobilized onto the GCE/L-Cys/AuNPs, the current response decreased due to the electronic repulsion between the negatively charged DNA and $[Fe(CN)_6]^{3-/4-}$ (curve d). After blocking with nonconductive HT, the peak current decreased again (curve e). As expected, because more negative charges have been introduced on the electrode surface, a further decreased response was observed after incubating with the S2 (curve f). After binding with the D-DOX-ABEI complex, peak current was dramatically inhibited and peak gap was significantly separated (curve g)，which was attributed to the largely increased negative charges of the DNA dendrimer.

Since EIS has been reported to be a very sensitive technique for characterizing electrode surface modification (Wang et al., 2016; Xie et al., 2016), we used this

technique to conform the construction process of the biosensor. Consistent with that observed in CV, Fig. 2B showed the impedance spectra at each modified steps. The L-Cys modified GCE showed a much larger impedance value (curve b) than bare GCE (curve a), then after AuNPs were electrodeposited on GCE/L-Cys, a decrease was observed (curve c). However, the impedance values were consecutively increased when S1 (curve d), HT (curve e), S2 (curve f) were incubated on the electrode. Subsequent assembling of D-DOX-ABEI complex caused the great increase (curve g). These results suggested that the ECL biosensor was successfully prepared.

Fig. 2.

3.3. Optimization of experimental conditions

H_2O_2 as the coreactant of luminol and its derivatives has great influence on the ECL efficiency (Xie et al., 2016; Wang et al., 2015; Jiang et al., 2016). To investigate the optimal concentration of H_2O_2, the ECL responses of the biosensor incubated with 10 ng/mL LN were recorded in different concentrations of H_2O_2. As shown in Fig. 2C, with the increase of H_2O_2 concentration, a consecutive increased ECL intensity was observed from 0 to 2 mM, while further increasing the concentration of H_2O_2 did not induce a significant enhancement of ECL signal. Therefore, the optimized concentration of H_2O_2 was 2 mM in the detection buffer.

Because Exo III-assisted target cyclic amplification played an important role in the ultrasensitive detection of LN. Therefore, it was required to ensure the optimized concentration of Exo III in this study and the results were shown in Fig. 2D. The proposed biosensor was assessed by different Exo III concentrations (0, 50, 100, 200,

300, 400 U/mL) at 10 ng/mL LN, and 60 min was chosen for enzymatic cleavage time. With an increase in the concentration of Exo III, the corresponding response increased. Then, a plateau was observed when the concentration of Exo III was more than 300 U/mL. Thus, the optimal concentration of Exo III was 300 U/mL, which was adopted in the subsequent work.

3.4. Possible luminescence mechanisms of the proposed ECL biosensor

To evaluate the effect of L-Cys on the response of the biosensor, we explored the ECL responses of the biosensor by depositing with or without L-Cys and the results were shown in Fig. 3A. Expectedly, an ECL signal about 5234 a.u. was observed when the GCE directly deposited with AuNPs (curve a). When the GCE was deposited with L-Cys and AuNPs simultaneously, an obvious increase of ECL response could be obtained about 8124 a.u. (curve b) in the presence of 10 ng/mL LN. The result indicated that L-Cys played an important role in the signal amplification of the ABEI-H_2O_2 ECL system. This phenomenon may be owing that a strong oxidation ability of L-Cys• which formed by loss an electron of L-Cys, could subsequently react with the oxidative intermediate of ABEI quickly to enhance ECL intensity. Moreover, it is well known that H_2O_2 is the most commonly used coreactant in ABEI system, the decomposition of H_2O_2 may generate a large number of reactive oxygen species (ROSs) to further oxidize ABEI for ECL emission (Xie et al., 2016; Liu et al., 2016; Du et al., 2014). In conclusion, the possible mechanisms were shown in Fig. 3B.

Fig. 3.

3.5. Analytical property of the ECL biosensor for LN detection

To investigate the potential performance and the sensitivity of the proposed biosensor, we detected various concentrations of LN using the prepared ECL biosensor under the optimal conditions. The Fig. 4A depicted the ECL intensity gradually increased (curves a-h) corresponding to increasing concentration of LN in the range of 0.1 pg/mL to 100 ng/mL. As shown in the Fig. 4B, the ECL signal was proportional to the logarithm (lg) of the concentration with a regression equation expressed as $I = 6702.6+1481.0 \lg c$ (I is the ECL peak intensity, c is the concentration of LN) and the correlation coefficient was $R = 0.9983$. The detection limit of 0.0661 pg/mL was estimated according to $3S_B/m$ (S_B means the standard deviation of the blank, m is the slope of the corresponding linear regression equation). Additionally, the analytical performance of the proposed biosensor was compared with previously reported LN detection methods (Table S2, see the Supporting Information). As the result, the proposed biosensor exhibited a lower detection limit than other approaches, which should be attributed to the large immobilized amount of Dox-ABEI complex and the recycling amplification of target protein. This suggested that the proposed biosensor is highly sensitive and has great potential for accurate detection of LN.

Fig. 4.

3.6. Reproducibility, stability and selectivity of the biosensor

Reproducibility, stability and selectivity are great importance to estimate the performance of the biosensor. Here, inter-assays precision was carried out to estimate

the reproducibility of this biosensor toward three concentrations (1 pg/mL, 0.1 ng/mL, and 10 ng/mL) of LN in different batches, and the relative standard deviations (RSD) were 6.2, 4.7, and 4.2% (n = 3) respectively, suggesting that the prepared biosensor had a good reproducibility. Moreover, stability is another important criterion for a biosensor. Hence, the stability of this ECL biosensor was investigated at various concentrations of LN. As shown in Fig. 4C, every concentration of LN presented a relatively stable curve which indicated that the proposed biosensor had an excellent stability. To further evaluate the selectivity and specificity of the proposed ECL biosensor, AFP (50 ng/mL), CEA (50 ng/mL) and Mucin1 (50 ng/mL) were chosen as interfering substances to construct contrast biosensor. According to Fig. 4D, no significant ECL signal of the AFP, CEA and Mucin1 was observed except that for target LN. Importantly, the ECL intensity of the mixture containing the above three interferents and LN exhibited a similar ECL signal to that obtained from the target LN only. These results indicated that the prepared biosensor possessed a good reproducibility, stability and selectivity for LN detection.

3.7. Application of the biosensor for the detection of LN

To investigate the viability of the proposed biosensor for application, lab study results of human serum samples (obtained from Chongqing General Hospital, prior to use, the serum was obtained by centrifugation clotted blood at 3000 rpm for 20 min, and then collected and stored at -20°C for further use.) were compared with those obtained by the commercial ECL immunoassay used in clinical diagnosis. As shown in Table 1, the data obtained by the proposed biosensor exhibited good consistency

with those detected by the commercial ECL immunoassay, demonstrating that the proposed ECL biosensor performed well reliability and provided a potential application for LN detection in clinical diagnosis.

Table 1

4. Conclusion

In summary, a proposed ECL biosensor based on DNA dendrimer-carried luminophore system and DNA nanomachine-mediated target recycling was fabricated for ultrasensitive detection of LN. This biosensor revealed two highlighted characteristics: (I) A DNA dendrimer was constructed by self-assembly of Y-shape DNA and cDNA, which provided sufficient intercalated sites for the efficient immobilization of massive ECL luminophores (ABEI) to improve the luminous efficiency remarkably. (II) A DNA nanomachine based on target antigen-attended DNA strand displacement and Exo III-assisted protein cyclic amplification was involved, by which a little of target protein (LN) input was converted into a large number of nucleic acid (S2) output to improve the sensitivity of detection. The testing results of LN from the proposed ECL biosensor were in good agreement with those from the commercial immunoassay. Taking these advantages into account, it could be expected that this proposed ECL biosensor will be significant for the early diagnosis and treatment of liver fibrosis, and may hold promising potential in biological analysis and clinical application.

Acknowledges

This work was financially supported by the National Natural Science Foundation of China (81572089), and the Chongqing Basic and Frontier Research (cstc2016jcyjA0177), China.

References

Bi, S., Chen, M., Jia, X.Q., Dong, Y., Wang, Z.H., 2015. Angew. Chem., Int. Ed. 54, 8144-8148.

Du, S.P., Guo, Z.Y., Chen, B.B., Sha, Y.H., Jiang, X.H., Li, X., Gan, N., Wang, S., 2014. Biosens. Bioelectron. 53, 135-141.

El-Mahdy, A.F., Shibata, T., Kabashima, T., Kai, M., 2014. Chem. Commun. 50, 859-861.

El-Mezayen, H.A., Habib, S., Marzok, H.F., Saad, M.H., 2015. Eur. J. Gastroenterol. Hepatol. 27, 378-385.

Endo, M., Katsuda, Y., Hidaka, K., Sugiyama, H., 2010. J. Am. Chem. Soc. 132, 1592-1597.

Jiang, X.Y., Wang, H.J., Wang, H.J., Zhuo, Y., Yuan, R., Chai, Y.Q., 2016. Nanoscale 8, 8017-8023.

Jiang, X.Y., Wang, H.J., Wang, H.J., Zhuo, Y., Yuan. R., Chai. Y.Q., 2017. Anal. Chem. 89, 4280-4286.

Jiang, X.Y., Wang, H.J., Yuan, R., Chai, Y.Q., 2015. Biosens. Bioelectron. 63, 33-38.

Kleinman, H.K., Cannon, F.B., Laurie, G.W., Hassell, J.R., Aumailley, M., Terranova, V.P., Martin, G.R., DuBois-Dalcq, M., 1985. J. Cell. Biochem. 27, 317-325.

Li, D.D., Cheng, W., Li, Y.J., Xu, Y.J., Li, X.M., Yin, Y.B., Ju, H.X., Ding, S.J., 2016. Anal. Chem. 88, 7500-7506.

Li, F., Zhu, C.L., Zhang, H., Huang, H., Wei, Q., Zhu, X., Cheng, X.Y., 2012. Braz. J. Infect. Dis. 16, 9-14.

Li, G.X., Yu, X.X., Liu, D.Q., Liu, X.Y., Li, F., Cui, H., 2015. Anal. Chem. 87, 10976-10981.

Liber, M., Tomov, T.E., Tsukanov, R., Berger, Y., Nir, E., 2015. Small 11, 568-575.

Liu, B.Q., Chen, J.F., Wei, Q.H., Zhang, B., Zhang, L., Tang, D.P., 2015. Biosens. Bioelectron. 2015, 69, 241-248.

Liu, H.Y., Lou, Y.B., Zhou, F., Zhu, H., Abdel-Halimd, E.S., Zhu, J.J., 2015. Biosens. Bioelectron. 71, 249-255.

Liu, Y.T., Wang, H.J., Xiong, C.Y., Yuan, Y.L., Chai, Y.Q., Yuan, R., 2016. Biosens. Bioelectron. 81,334-340.

Lund, K., Manzo, A.J., Dabby, N., Michelotti, N., Johnson-Buck, A., Nangreave, J., Taylor, S., Pei, R., Stojanovic, M.N., Walter, N.G., Winfree, E., Yan, H., 2010. Nature 465, 206-210.

Meng, H.M., Zhang, X.B., Lv, Y.F., Zhao, Z.L., Wang, N.N., Fu, T., Fan, H.H., Liang, H., Qiu, L.P., Zhu, G.Z., Tan, W.H., 2014. ACS Nano 8, 6171-6181.

Mohammed, A.M., Schulman, R., 2013. Nano Lett. 13, 4006-4013.

Muscat, R.A., Bath, J., Turberfield, A. J., 2012. Small 8, 3593-3597.

Rodin, S., Domogatskaya, A., Ström, S., Hansson, E.M., Chien, K.R., Inzunza, J., Hovatta, O., Tryggvason, K., 2010. Nat. Biotechnol. 28, 611-615.

Sadowski, J.P., Calvert, C.R., Zhang, D.Y., Pierce, N.A., Yin, P., 2014. ACS Nano 8, 3251-3259.

Valkonen, K.H., Ringner, M., Ljungh, A., Wadström, T., 1993. FEMS. Immunol. Med. Microbiol. 7, 29-37.

Wang, F., Liu, X,Q., Willner, I., 2015. Angew. Chem. Int. Ed. 54, 1098-1129.

Wang, H.J., Yuan. Y.L., Zhuo. Y., Chai, Y.Q., Yuan, R., 2016. Anal. Chem. 88, 5797-5803.

Wang, J.X., Zhuo, Y., Zhou, Y., Yuan, R., Chai, Y.Q., 2015. Biosens. Bioelectron. 71, 407-413.

Wang, L.J., Zhang, Y., Zhang, C.Y., 2013. Anal. Chem. 85, 11509-11517.

Wu, F.F., Zhou, Y., Wang, J.X., Zhuo, Y., Yuan, R., Chai, Y.Q., 2016. Sens. Actuators B 243, 1067-1074.

Xie, S.B., Dong, Y., Yuan, Y., Chai, Y.Q., Yuan, R., 2016. Anal. Chem. 88, 5218-5224.

Xu, J.G., Wu, Z.S., Shen, W.Y., Xu, H., Li, H.L., Jia, L., 2015. Biosens. Bioelectron. 73, 19-25.

Yang, X.L., Tang, Y.N., Mason, S.D., Chen, J.B., Li, F., 2016. ACS Nano 10, 2324-2330.

Yang, Z.H., Zhuo, Y., Yuan, R., Chai, Y.Q., 2016. Anal. Chem. 88, 5189-5196.

Zhang, A., Xiang, H.K., Zhang, X., Guo, W.W., Yuan, E.H., Huang, C.S., Jia, N.Q., 2016. Biosens. Bioelectron. 75, 206-212.

Zhang, H., Lai, M., Zuehlke, A., Peng, H., Li, X.F., Le, X.C., 2015. Angew. Chem. Int. Ed. 54, 14326-14330.

Zhang, H., Ma, Y., Xie, Y., An, Y., Huang, Y., Zhu, Z., Yang, C.J., 2015. Sci. Rep. 5, 10099-10107.

Zhang, H.L., Han, Z.L., Wang, X., Li, F., Cui, H., Yang, D., Bian, Z.P., 2015. ACS Appl. Mater. Interfaces 7, 7599-7604.

Zhang, J., Yuan, Y.L., Xie, S.B., Chai, Y.Q., Yuan, R., 2014. Biosens. Bioelectron. 60, 224-230.

Zhao, Y., Wang, H.M., Tang, W., Hu, S.C., Li, N., Liu, F., 2015. Chem. Commun. 51, 10660-10663.

Zhou, C., Yang, Z.Q., Liu, D.S., 2012. J. Am. Chem. Soc. 134, 1416-1418.

Zhou, T., Chen, P., Niu, L., Jin, J., Liang, D.H., Li, Z.B., Yang, Z.Q., Liu, D.S., 2012. Angew. Chem., Int. Ed. 51, 11271-11274.

Zhou, X.M., Zhu, D.B., Liao, Y.H., Liu, W.P., Liu, H.X., Ma, Z.K., Xing, D., 2014. Nat. Protoc. 9, 1146-1159.

Zhu, D.B., Zhou, X.M., Xing, D., 2010. Biosens. Bioelectron. 26, 285-288.

Zhu, D.B., Zhou, X.M., Xing, D., 2012. Anal. Chim. Acta 725, 39-43.

Zhu, G.Z., Hu, R., Zhao, Z.L., Chen, Z., Zhang, X.B., Tan, W.H., 2013. J. Am. Chem. Soc. 135, 16438-16445.

Zong, C., Wu, J., Liu, M.M., Yan, F., Ju, H.X., 2015. Chem. Sci. 6, 2602-2607.

BIOS 10034

Article reference: BIOS_BIOS-D-17-02156

Figure Captions

Scheme 1. (A) Preparation of the ECL probe D-Dox-ABEI. (B) Fabrication of an immunoreaction-induced DNA nanomachine. (C) Fabrication process of the ECL biosensor for LN detection based on DNA dendrimer and DNA nanomachine.

Fig. 1. (A). PAGE analysis of different DNA structure: lane 1, DNA; lane 2, Y1 (Y-shaped single-stranded DNA); lane 3, cDNA; lane 4, Y2 (Y-shaped single-stranded cDNA); lane 5, D (DNA dendrimer). (B) AFM and (C) SEM image of the DNA dendrimer.

Fig. 2. CV (A) and EIS (B) characterization of electrode at different modified stages: (a) bare GCE; (b) GCE/L-Cys; (c) GCE/L-Cys/AuNPs; (d) GCE/L-Cys/AuNPs/S1; (e) GCE/L-Cys/AuNPs/S1/HT; (f) GCE/L-Cys/AuNPs/S1/HT/S2; (g) GCE/L-Cys/AuNPs/S1/HT/S2/D-DOX-ABEI. Detection buffer: 2 mL of $[Fe(CN)_6]^{3-/4-}$ (5 mM, pH 7.0). (C). Influence of the concentration of H_2O_2 on the biosensor. (D). Influence of the concentration of Exo III on the biosensor. All the ECL intensity was detected with 10 ng/mL LN in 2 mL of PBS (pH 8.0).

Fig. 3. (A). ECL intensity of the biosensor without (a) or with (b) L-Cys in 2 mL of PBS

(pH 8.0) containing 2 mM H_2O_2. (B). The probable mechanism of the proposed ECL biosensor.

Fig. 4. (A). ECL intensity of the biosensor incubated with different concentrations of LN (a-h): 0.1 pg/mL, 1 pg/mL, 10 pg/mL, 0.1 ng/mL, 1 ng/mL, 10 ng/mL, 50 ng/mL, and 100 ng/mL. (B). Calibration plot of ECL intensity *vs* the logarithm of LN concentration. (C). The ECL stability of the proposed biosensor at various concentrations of LN. (D). The specificity evaluation of the ECL biosensor: Blank, AFP (50 ng/mL), CEA (50 ng/mL), Mucin 1 (50 ng/mL), LN (10 ng/mL), and a mixture containing AFP (50 ng/mL), CEA (50 ng/mL), Mucin 1 (50 ng/mL), LN (10 ng/mL).

Table 1. LN Detection in Human Serum with the proposed ECL Biosensor and commercial ECL immunoassay

Scheme 1

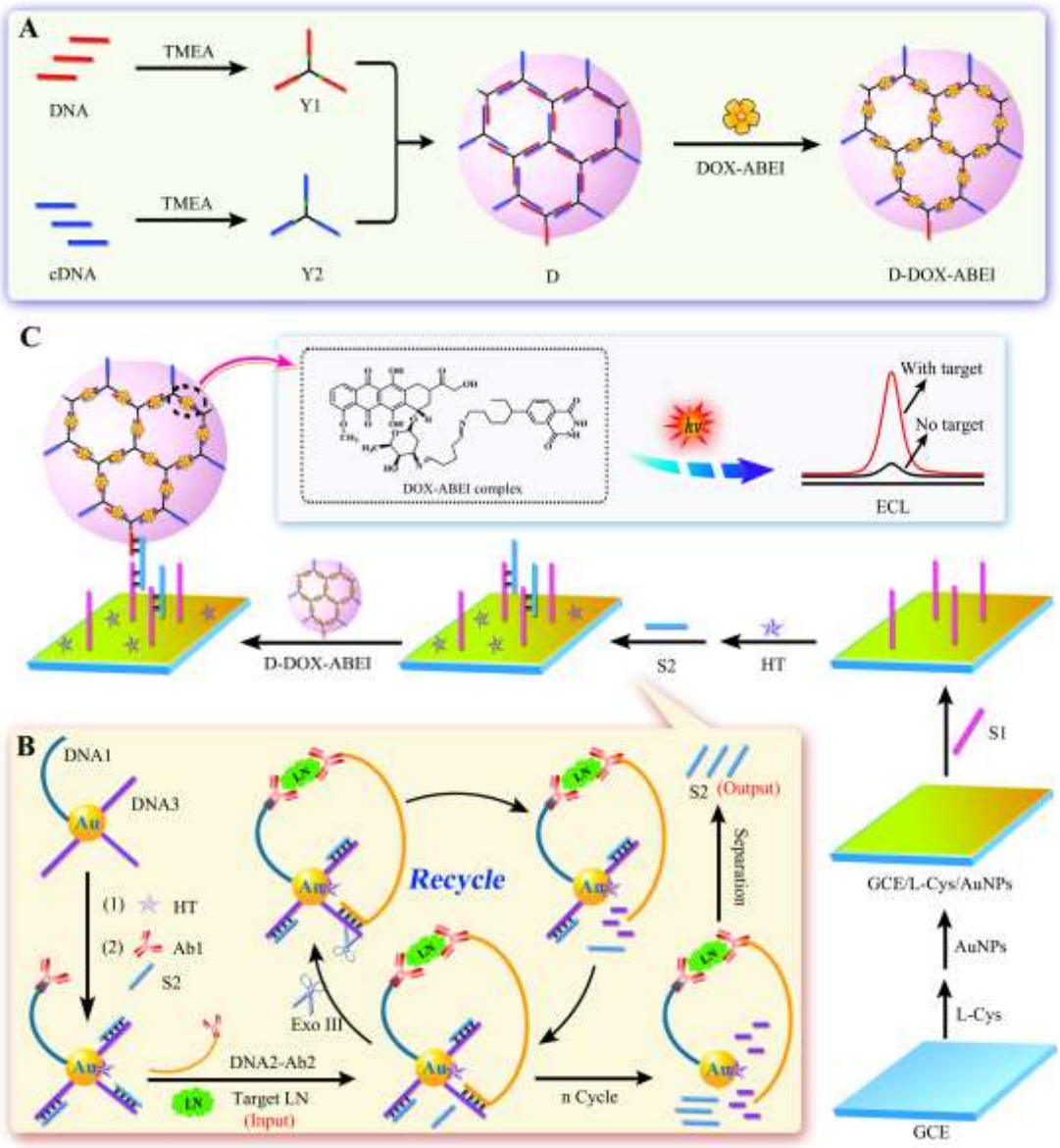

Scheme 1. (A) Preparation of the ECL probe D-Dox-ABEI. (B) Fabrication of an immunoreaction-induced DNA nanomachine. (C) Fabrication process of the ECL biosensor for LN detection based on DNA dendrimer and DNA nanomachine.

Fig. 1

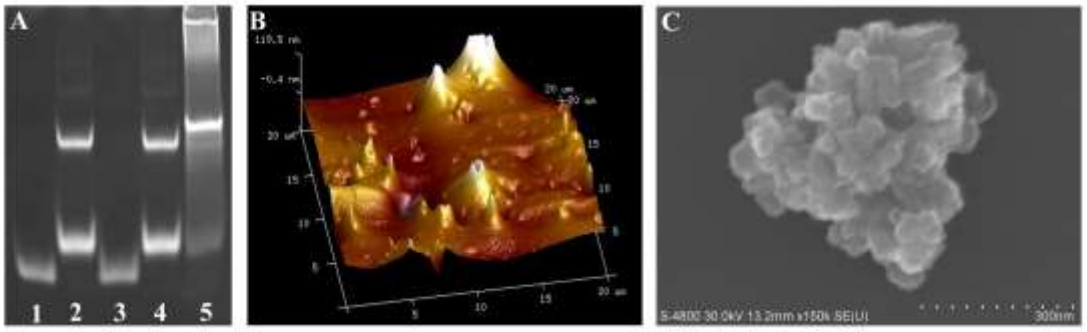

Fig. 1. (A). PAGE analysis of different DNA structure: lane 1, DNA; lane 2, Y1 (Y-shaped single-stranded DNA); lane 3, cDNA; lane 4, Y2 (Y-shaped single-stranded cDNA); lane 5, D (DNA dendrimer). (B) AFM and (C) SEM image of the DNA dendrimer.

Fig. 2

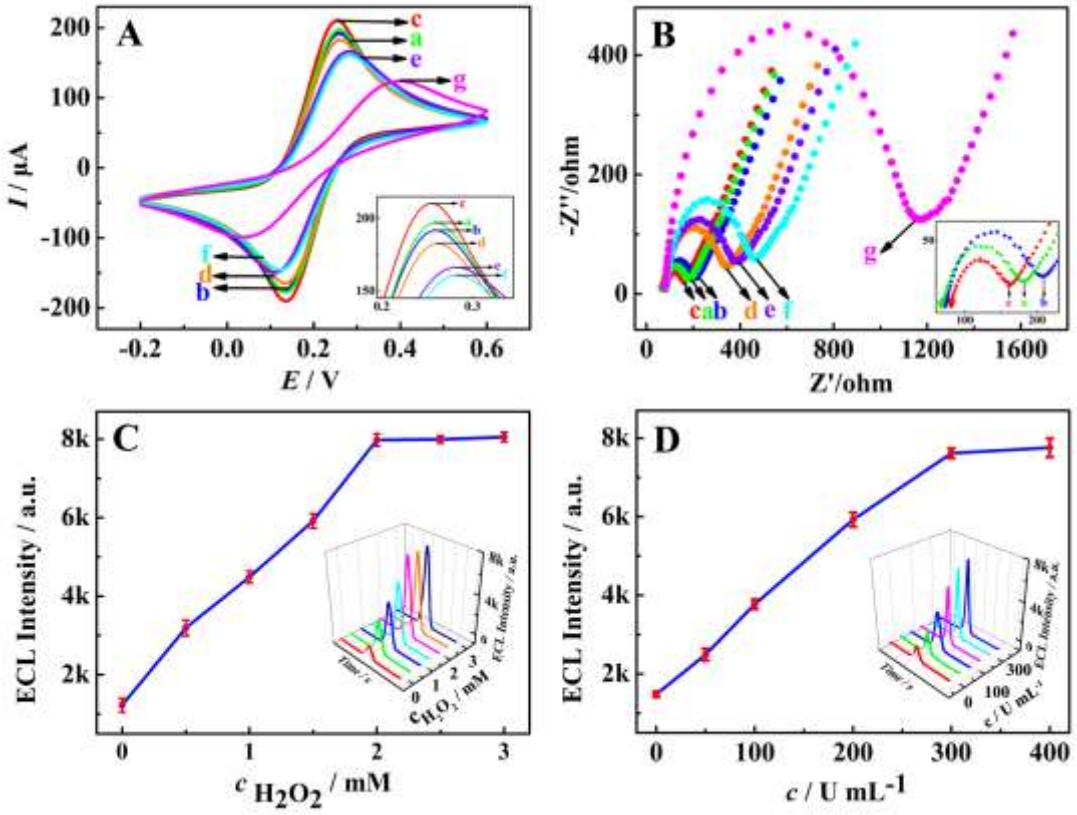

Fig. 2. CV (A) and EIS (B) characterization of electrode at different modified stages: (a) bare GCE; (b) GCE/L-Cys; (c) GCE/L-Cys/AuNPs; (d) GCE/L-Cys/AuNPs/S1; (e) GCE/L-Cys/AuNPs/S1/HT; (f) GCE/L-Cys/AuNPs/S1/HT/S2; (g) GCE/L-Cys/AuNPs/S1/HT/S2/D-DOX-ABEI. Detection buffer: 2 mL of $[Fe(CN)_6]^{3-/4-}$ (5 mM, pH 7.0). (C). Influence of the concentration of H_2O_2 on the biosensor. (D). Influence of the concentration of Exo III on the biosensor. All the ECL intensity was detected with 10 ng/mL LN in 2 mL of PBS (pH 8.0).

Fig. 3

Fig. 3. (A). ECL intensity of the biosensor without (a) or with (b) L-Cys in 2 mL of PBS (pH 8.0) containing 2 mM H_2O_2. (B). The probable mechanism of the proposed ECL biosensor.

Fig. 4

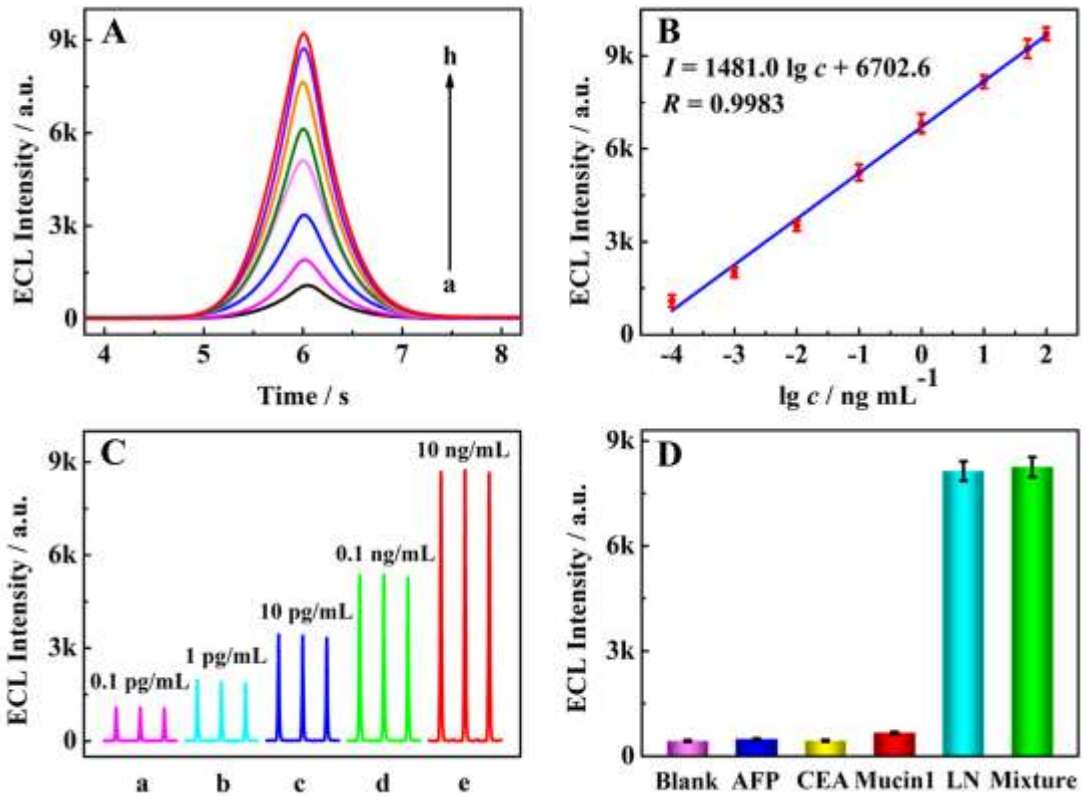

Fig. 4. (A). ECL intensity of the biosensor incubated with different concentrations of LN (a-h): 0.1 pg/mL, 1 pg/mL, 10 pg/mL, 0.1 ng/mL, 1 ng/mL, 10 ng/mL, 50 ng/mL, and 100 ng/mL. (B). Calibration plot of ECL intensity *vs* the logarithm of LN concentration. (C). The ECL stability of the proposed biosensor at various concentrations of LN. (D). The specificity evaluation of the ECL biosensor: Blank, AFP (50 ng/mL), CEA (50 ng/mL), Mucin 1 (50 ng/mL), LN (10 ng/mL), and a mixture containing AFP (50 ng/mL), CEA (50 ng/mL), Mucin 1 (50 ng/mL), LN (10 ng/mL).

Table 1 LN Detection in Human Serum with the proposed ECL Biosensor and commercial ECL immunoassay

samples	our method / ng mL^{-1}	commercial method / ng mL^{-1}	Relative error (%)
1	4.7	5.5	-14.5
2	23.4	27.0	-13.3
3	61.0	58.5	4.3
4	75.3	72.8	3.4
5	81.0	85.0	-4.7

Highlights

- The DNA dendrimer achieved high efficiency immobilization of ECL luminophore.
- The use of TMEA improved the synthetic efficiency of DNA dendrimer.
- A nanomachine-mediated recycling amplification improved the sensitivity of detection.